Available online at www.sciencedirect.com
SCIENCE DIRECT®
Physics Letters B 578 (2004) 45–53
PHYSICS LETTERS B
www.elsevier.com/locate/physletb

First measurement of the double-inclusive $B/\overline{B}$ hadron energy distribution in e^+e^- annihilations, and of angle-dependent moments of the B and $\overline{B}$ energies

SLD Collaboration

Koya Abe [y], Kenji Abe [o], T. Abe [v], I. Adam [v], H. Akimoto [v], D. Aston [v], K.G. Baird [k], C. Baltay [ae], H.R. Band [ad], T.L. Barklow [v], J.M. Bauer [l], G. Bellodi [q], R. Berger [v], G. Blaylock [k], J.R. Bogart [v], G.R. Bower [v], J.E. Brau [p], M. Breidenbach [v], W.M. Bugg [x], D. Burke [v], T.H. Burnett [ac], P.N. Burrows [s], A. Calcaterra [h], R. Cassell [v], A. Chou [v], H.O. Cohn [x], J.A. Coller [d], M.R. Convery [v], V. Cook [ac], R.F. Cowan [m], G. Crawford [v], C.J.S. Damerell [t], M. Daoudi [v], N. de Groot [b], R. de Sangro [h], D.N. Dong [m], M. Doser [v], R. Dubois, I. Erofeeva [n], V. Eschenburg [l], E. Etzion [ad], S. Fahey [e], D. Falciai [h], J.P. Fernandez [aa], K. Flood [k], R. Frey [p], E.L. Hart [x], K. Hasuko [y], S.S. Hertzbach [k], M.E. Huffer [v], X. Huynh [v], M. Iwasaki [p], D.J. Jackson [t], P. Jacques [u], J.A. Jaros [v], Z.Y. Jiang [v], A.S. Johnson [v], J.R. Johnson [ad], R. Kajikawa [o], M. Kalelkar [u], H.J. Kang [u], R.R. Kofler [k], R.S. Kroeger [l], M. Langston [p], D.W.G. Leith [v], V. Lia [m], C. Lin [k], G. Mancinelli [u], S. Manly [ae], G. Mantovani [r], T.W. Markiewicz [v], T. Maruyama [v], A.K. McKemey [c], R. Messner [v], K.C. Moffeit [v], T.B. Moore [ae], M. Morii [v], D. Muller [v], V. Murzin [n], S. Narita [y], U. Nauenberg [e], H. Neal [ae], G. Nesom [q], N. Oishi [o], D. Onoprienko [x], L.S. Osborne [m], R.S. Panvini [ab], C.H. Park [w], I. Peruzzi [h], M. Piccolo [h], L. Piemontese [g], R.J. Plano [u], R. Prepost [ad], C.Y. Prescott [v], B.N. Ratcliff [v], J. Reidy [l], P.L. Reinertsen [aa], L.S. Rochester [v], P.C. Rowson [v], J.J. Russell [v], O.H. Saxton [v], T. Schalk [aa], B.A. Schumm [aa], J. Schwiening [v], V.V. Serbo [v], G. Shapiro [j], N.B. Sinev [p], J.A. Snyder [ae], H. Staengle [f], A. Stahl [v], P. Stamer [u], H. Steiner [j], D. Su [v], F. Suekane [y], A. Sugiyama [o], A. Suzuki [o], M. Swartz [i], F.E. Taylor [m], J. Thom [v], E. Torrence [m], T. Usher [v], J. Va'vra [v], R. Verdier [m], D.L. Wagner [e], A.P. Waite [v], S. Walston [p], A.W. Weidemann [x], E.R. Weiss [ac], J.S. Whitaker [d], S.H. Williams [v], S. Willocq [k], R.J. Wilson [f], W.J. Wisniewski [v], J.L. Wittlin [k], M. Woods [v], T.R. Wright [ad], R.K. Yamamoto [m], J. Yashima [y], S.J. Yellin [z], C.C. Young [v], H. Yuta [a]

[a] *Aomori University, Aomori 030, Japan*
[b] *University of Bristol, Bristol, United Kingdom*

doi:10.1016/j.physletb.2003.10.057

[c] Brunel University, Uxbridge, Middlesex UB8 3PH, United Kingdom
[d] Boston University, Boston, MA 02215, USA
[e] University of Colorado, Boulder, CO 80309, USA
[f] Colorado State University, Ft. Collins, CO 80523, USA
[g] INFN Sezione di Ferrara and Universita di Ferrara, I-44100 Ferrara, Italy
[h] INFN Laboratori Nazionali di Frascati, I-00044 Frascati, Italy
[i] Johns Hopkins University, Baltimore, MD 21218-2686, USA
[j] Lawrence Berkeley Laboratory, University of California, Berkeley, CA 94720, USA
[k] University of Massachusetts, Amherst, MA 01003, USA
[l] University of Mississippi, University, MS 38677, USA
[m] Massachusetts Institute of Technology, Cambridge, MA 02139, USA
[n] Institute of Nuclear Physics, Moscow State University, 119899 Moscow, Russia
[o] Nagoya University, Chikusa-ku, Nagoya 464, Japan
[p] University of Oregon, Eugene, OR 97403, USA
[q] Oxford University, Oxford OX1 3RH, United Kingdom
[r] INFN Sezione di Perugia and Universita di Perugia, I-06100 Perugia, Italy
[s] Queen Mary, University of London, London E1 4NS, United Kingdom
[t] Rutherford Appleton Laboratory, Chilton, Didcot, Oxon OX11 0QX, United Kingdom
[u] Rutgers University, Piscataway, NJ 08855, USA
[v] Stanford Linear Accelerator Center, Stanford University, Stanford, CA 94309, USA
[w] Soongsil University, Seoul 156-743, South Korea
[x] University of Tennessee, Knoxville, TN 37996, USA
[y] Tohoku University, Sendai 980, Japan
[z] University of California at Santa Barbara, Santa Barbara, CA 93106, USA
[aa] University of California at Santa Cruz, Santa Cruz, CA 95064, USA
[ab] Vanderbilt University, Nashville, TN 37235, USA
[ac] University of Washington, Seattle, WA 98105, USA
[ad] University of Wisconsin, Madison, WI 53706, USA
[ae] Yale University, New Haven, CT 06511, USA

Received 18 September 2003; received in revised form 10 October 2003; accepted 15 October 2003

Editor: H. Weerts

Abstract

We have made the first measurement of the double-inclusive $B/\overline{B}$ energy distribution in e^+e^- annihilations, using a sample of 400 000 hadronic Z^0-decay events recorded in the SLD experiment at SLAC between 1996 and 1998. The small and stable SLC beam spot and the CCD-based vertex detector were used to reconstruct $B/\overline{B}$-decay vertices with high efficiency and purity, and to provide precise measurements of the kinematic quantities used to calculate the B energies in this novel technique. We measured the $B/\overline{B}$ energies with good efficiency and resolution over the full kinematic range. We measured moments of the scaled energies of the B and $\overline{B}$ hadrons vs. the opening angle between them. By comparing these results with perturbative QCD predictions we tested the ansatz of factorisation in heavy-quark production. A recent next-to-leading order calculation reproduces the data.

1. Introduction

The production of heavy hadrons (H) in e^+e^- annihilation provides a laboratory for the study of heavy-quark (Q) jet fragmentation. This is commonly char-

E-mail address: p.burrows@qmul.ac.uk (P.N. Burrows).

acterized in terms of the observable $x_H \equiv 2E_H/\sqrt{s}$, where E_H is the energy of a B or D hadron containing a b or c quark, respectively, and $\sqrt{s}$ is the c.m. energy. The distribution of x_H, $D(x_H)$, is conventionally referred to as the heavy-quark 'fragmentation function'.[1]

In recent publications we presented [1,2] the results of a new method for reconstructing B-hadron decays, and the B energy, inclusively, using only charged tracks, in the SLD experiment at SLAC. We used the upgraded charge-coupled device (CCD) vertex detector, installed in 1996, to reconstruct B-decay vertices in Z^0 decays with high efficiency and purity. Combined with the micron-sized SLC interaction point (IP), our precise vertexing allowed us to reconstruct the total transverse momentum of the tracks from B-decays, and therefore the transverse momentum and mass associated with the neutral particles in the B-decays. This allowed us to reconstruct accurately the energy of B hadrons. These studies yielded the most precise measurement of the b-quark fragmentation function, and allowed us to test models of heavy-quark fragmentation. Of the 9 models tested, only 4 were consistent with our precision data at better than the 1% level based on a χ^2 probability. This allowed us to reduce the model-dependent systematic uncertainty on the b-quark fragmentation function.

We have extended these studies and applied similar 'topological' vertexing techniques to tag events in which we reconstructed the energies of both leading B hadrons produced via $e^+e^- \to b\bar{b} \to B\overline{B} + X$. We measured the moments of the single-inclusive B-hadron scaled-energy distribution dN/dx_B:

$$D_i \equiv \int x_B^{i-1} \frac{1}{N_s} \frac{dN_s}{dx_B}\, dx_B \tag{1}$$

as well as the moments of the double-inclusive scaled-energy distribution:

$$D_{ij}(\phi) \equiv \iint x_{B1}^{i-1} x_{B2}^{j-1} \frac{1}{N_d} \frac{d^3N_d}{dx_{B1}\, dx_{B2}\, d\cos\phi}\, dx_{B1}\, dx_{B2}, \tag{2}$$

where x_{B1} and x_{B2} are the scaled energies of the two B hadrons and the label is arbitrary, ϕ is the angle between their flight directions, and i and j are integers $\geqslant 1$. We formed the normalised moments:

$$G_{ij}(\phi) \equiv D_{ij}(\phi)/(D_i D_j). \tag{3}$$

Following the method proposed in [3] we used these quantities to test the ansatz of factorisation as applied to perturbative quantum chromodynamics (pQCD) calculations of $e^+e^- \to b\bar{b}$ events.

Due to 'soft', or non-perturbative, effects, D_i and D_{ij} cannot be predicted absolutely in pQCD. Rather, the respective pQCD calculation must be folded with models of the non-perturbative ('hadronisation') process in order to derive predictions that can be compared with experimental data. However, provided that the ansatz of factorisation holds [3], namely that calculation of the perturbative and non-perturbative phases can be separated by (an arbitrary) factorisation scale μ_F, the dependence on μ_F cancels in Eq. (3) and hence G_{ij} can be calculated absolutely in pQCD, up to possible 'higher twist' effects of order $1/\sqrt{s}$, with no dependence on hadronisation models. Comparison of the measured G_{ij} with pQCD predictions hence allows both a test of this ansatz and of the perturbative calculations. The G_{ij} can be derived at leading order (LO) in pQCD using the numerical results in [3]. In addition, next-to-leading order (NLO) predictions for G_{ij} have been calculated recently [4].

In Section 2 we describe the detector and the selection of $e^+e^- \to$ hadrons events used in this analysis. We present in Section 3 the first measurement of the double-inclusive B-hadron energy distribution and, in Section 4, of the normalised moments Eq. (3). In Section 5 we describe the estimation of the errors on our measurements. Finally, in Section 6, we test the ansatz of factorisation and compare our data with the pQCD predictions.

2. Apparatus and hadronic event selection

This analysis is based on roughly 400 000 hadronic Z^0 events produced in e^+e^- annihilations at a mean center-of-mass energy of $\sqrt{s} = 91.28$ GeV at the SLAC Linear Collider (SLC), and recorded in the SLC Large Detector (SLD) between 1996 and 1998. A general description of the SLD can be found

[1] Unless stated otherwise, in these studies we do not distinguish between hadrons and antihadrons.

elsewhere [5]. The trigger and initial selection criteria for hadronic Z^0 decays are described in Ref. [6]. This analysis used charged tracks measured in the Central Drift Chamber (CDC) [7] and in the upgraded Vertex Detector (VXD3) [8]. Momentum measurement was enabled by a uniform axial magnetic field of 0.6 T. The CDC and VXD3 gave a momentum resolution of $\sigma_{p_\perp}/p_\perp = 0.01 \oplus 0.0026\, p_\perp$, where $p_\perp$ is the track momentum transverse to the beam axis in GeV/c. In the plane normal to the beamline the centroid of the micron-sized SLC IP was reconstructed from tracks in sets of approximately thirty sequential hadronic Z^0 decays to a precision of $\sigma_{\rm IP}^{r\phi} \simeq 4$ μm. The IP position along the beam axis was determined event by event, using charged tracks, with a resolution of $\sigma_{\rm IP}^{z} \simeq 20$ μm. Including the uncertainty on the IP position, the resolution on the charged-track impact parameter (d) projected in the plane perpendicular to the beamline was $\sigma_d^{r\phi} = 8 \oplus 33/(p \sin^{3/2}\theta)$ μm, and the resolution in the plane containing the beam axis was $\sigma_d^{z} = 10 \oplus 33/(p \sin^{3/2}\theta)$ μm, where θ is the track polar angle with respect to the beamline.

A set of cuts was applied to the data to select well-measured tracks and events well contained within the detector acceptance. Charged tracks were required to have a distance of closest approach transverse to the beam axis within 5 cm, and within 10 cm along the axis from the measured IP, as well as $|\cos\theta| < 0.87$, and $p_\perp > 0.15$ GeV/c. Events were required to have a minimum of five such tracks, a thrust axis [9] polar angle w.r.t. the beamline, θ_T, within $|\cos\theta_T| < 0.80$, and a charged visible energy $E_{\rm vis}$ of at least 20 GeV, which was calculated from the selected tracks assigned the charged pion mass. The efficiency for selecting a well-contained $Z^0 \to q\bar{q}(g)$ event was estimated to be above 97% independent of quark flavor. The selected sample comprised 313 447 events, with an estimated 0.10 ± 0.05% background contribution dominated by $Z^0 \to \tau^+\tau^-$ events.

For the purpose of estimating the efficiency and purity of the selection procedures we made use of a detailed Monte Carlo (MC) simulation of the detector. The JETSET 7.4 [10] event generator was used, with parameter values tuned to hadronic e^+e^- annihilation data [11], combined with a simulation of B-hadron decays tuned [12] to $\Upsilon(4S)$ data and a simulation of the SLD based on GEANT 3.21 [13]. Inclusive distributions of single-particle and event-topology observables in hadronic events were found to be well described by the simulation [6]. Uncertainties in the simulation were taken into account in the systematic errors (Section 5).

3. B-hadron selection and energy measurement

The event sample for this analysis was selected using a 'topological' vertexing technique based on the detection and measurement of charged tracks, which is described in detail in Refs. [14–16]. We considered events in which we found decay vertices corresponding to both the leading B and $\overline{B}$ hadrons. First, the Durham algorithm [17] was applied to the selected hadronic events, with a y_c parameter value of 0.015, in order to define a jet structure in each event. We found that this algorithm and y_c value minimized the number of B (and D) decay tracks assigned to the wrong jet. This is an important feature for our analysis because we used vertex-related variables derived only from charged tracks. Events containing 2, 3, or 4 jets were retained for further analysis.

In each selected event, the vertexing algorithm was applied to the set of tracks in each jet. Vertices consistent with photon conversions or K^0 or Λ^0 decays were discarded. Events were retained in which a vertex was found in exactly two jets. 35 137 events were selected, of which 89.4% were estimated to be of $b\bar{b}$ origin. The efficiency for selecting true $b\bar{b}$ events was estimated to 36.3%.

The large masses of the B hadrons relative to light-flavor hadrons make it possible to distinguish B-hadron decay vertices from those vertices found in events of lighter flavors using the vertex invariant mass, M. However, due to those particles missed from the vertex, which are mainly neutrals, M cannot be fully determined. M can be written

$$M = \sqrt{M_{\rm ch}^2 + P_{\rm t}^2 + P_{{\rm ch}l}^2} + \sqrt{M_0^2 + P_{\rm t}^2 + P_{0l}^2}, \qquad (4)$$

where $M_{\rm ch}$ and M_0 are the total invariant masses of the set of vertex-associated tracks and the set of missing particles, respectively. $P_{\rm t}$ is the total charged-track momentum transverse to the B flight direction, which, by momentum conservation, is identical to the transverse momentum of the set of missing particles. $P_{{\rm ch}l}$ and P_{0l} are the respective momenta along the B

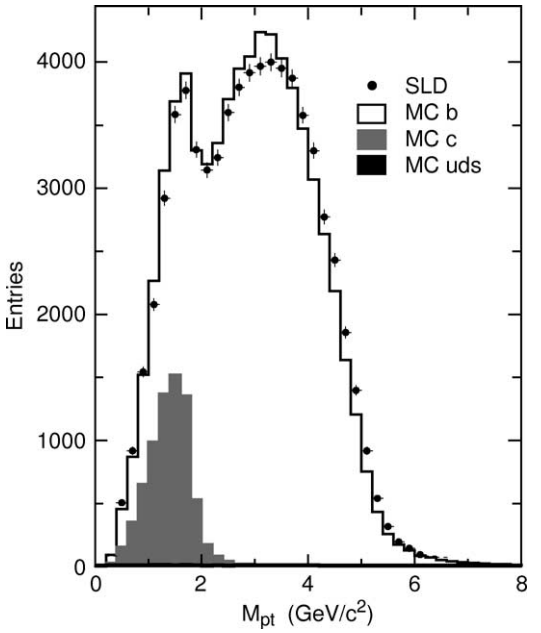

Fig. 1. P_t-corrected mass (see text); data (points) compared with the simulation (histograms) in which the primary flavor content is indicated. The contribution from *uds* events is barely visible above the horizontal axis.

flight direction, which we take to be the vector joining the IP to the vertex.

The lower bound for the mass of the decaying hadron, the 'P_t-corrected vertex mass' [2],

$$M_{\mathrm{Pt}} = \sqrt{M_{\mathrm{ch}}^2 + P_{\mathrm{t}}^2} + |P_{\mathrm{t}}| \tag{5}$$

was used as the variable for selecting B hadrons. Fig. 1 shows the distribution of M_{Pt} for vertices in the selected event sample, and the corresponding simulated distribution. Events were selected that contained at least one vertex with $M_{\mathrm{Pt}} > 2.0$ GeV/c^2 and $M_{\mathrm{Pt}} \leqslant 2 \times M_{\mathrm{ch}}$. The latter cut was found to reduce the contamination from fake vertices in light-quark events.

In order to improve the $b\bar{b}$ purity of the sample, events were selected in which both vertices had a flight length, d_{vtx}, such that $0.1 < d_{\mathrm{vtx}} < 2.3$ cm; in which at least one vertex contained two 'significant' tracks, i.e., tracks with a normalised impact-parameter significance, d/σ_d, of at least 2 units; and in which the angle between the vertex flight vectors, ϕ, satisfied $\cos\phi < 0.99$. The last cut was effective at removing events in which either a gluon had split into heavy quarks, or the jet-finder had artificially split a single heavy-quark jet into two jets.

The energy of each B hadron, E_B, can be expressed as the sum of the reconstructed-vertex energy, E_{ch}, and the energy of those particles not associated with the vertex, E_0. We can write

$$E_0^2 = M_0^2 + P_{\mathrm{t}}^2 + P_{0l}^2. \tag{6}$$

The two unknowns, M_0 and P_{0l}, must be found in order to obtain E_0. One kinematic constraint can be obtained by imposing the B-hadron mass on the vertex, $M_B^2 = E_B^2 - P_B^2$, where $P_B = P_{\mathrm{ch}l} + P_{0l}$ is the total momentum of the B hadron. From Eq. (4) we derive the following inequality,

$$\sqrt{M_{\mathrm{ch}}^2 + P_{\mathrm{t}}^2} + \sqrt{M_0^2 + P_{\mathrm{t}}^2} \leqslant M_B, \tag{7}$$

where equality holds in the limit where both P_{0l} and $P_{\mathrm{ch}l}$ vanish in the B-hadron rest frame. Eq. (7) effectively sets an upper bound on M_0, and a lower bound is given by zero

$$0 \leqslant M_0^2 \leqslant M_{0\,\mathrm{max}}^2, \tag{8}$$

where

$$M_{0\,\mathrm{max}}^2 = M_B^2 - 2M_B\sqrt{M_{\mathrm{ch}}^2 + P_{\mathrm{t}}^2} + M_{\mathrm{ch}}^2. \tag{9}$$

Because M_0 peaks near $M_{0\,\mathrm{max}}$, [15] we set $M_0^2 = M_{0\,\mathrm{max}}^2$ if $M_{0\,\mathrm{max}}^2 \geqslant 0$, and $M_0^2 = 0$ if $M_{0\,\mathrm{max}}^2 < 0$. We calculated P_{0l}:

$$P_{0l} = \frac{M_B^2 - (M_{\mathrm{ch}}^2 + P_{\mathrm{t}}^2) - (M_0^2 + P_{\mathrm{t}}^2)}{2(M_{\mathrm{ch}}^2 + P_{\mathrm{t}}^2)} P_{\mathrm{ch}l}, \tag{10}$$

and hence E_0 (Eq. (6)). We then reconstructed the B-hadron energy, $E_B^{\mathrm{rec}} = E_0 + E_{\mathrm{ch}}$. Events were retained in which both reconstructed B energies satisfied $E_B^{\mathrm{rec}} < 60$ GeV. A final sample of 19 809 events was obtained with an estimated $b\bar{b}$ selection efficiency of 21.7% and a background contribution of only 0.23%, which was almost entirely from $Z^0 \to c\bar{c}$ events.

The energy resolution of the final B sample is shown in Fig. 2, where we plot the normalised residual on E_B: $(E_B^{\mathrm{true}} - E_B^{\mathrm{rec}})/E_B^{\mathrm{true}}$. The distribution was fitted to a double Gaussian function for which the mean positions, widths and normalisations were allowed to vary. 79.5% of the population lies in the 'core' Gaussian, of width 21.3%; the remaining population is characterised by a 'tail' Gaussian of width 31.3%.

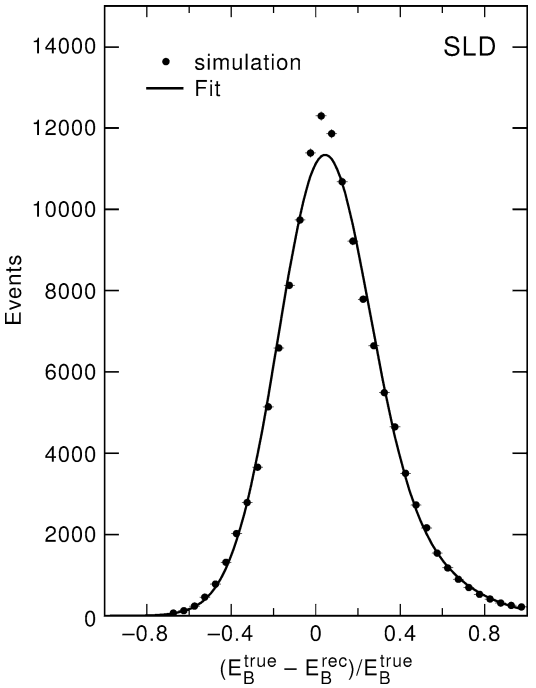

Fig. 2. Resolution on the reconstructed B-hadron energy.

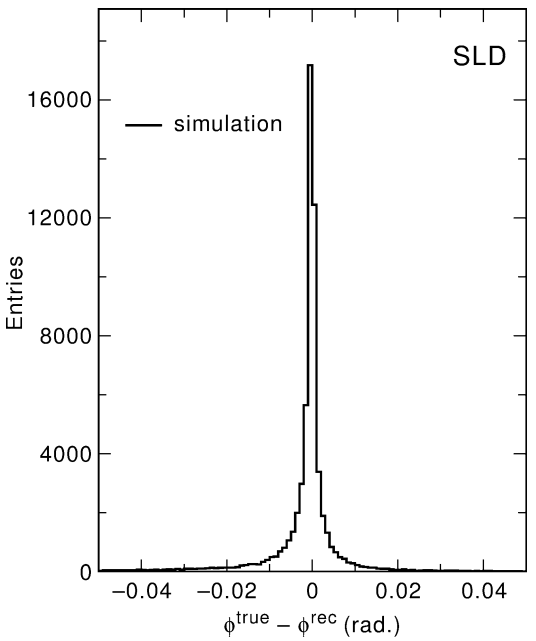

Fig. 3. Resolution on the reconstructed angle between the two B hadrons.

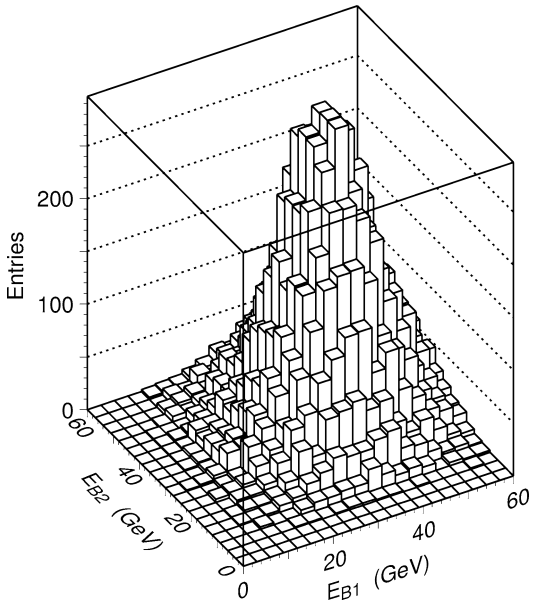

Fig. 4. Reconstructed double-inclusive B-hadron energy distribution.

The angular resolution was similarly investigated and is shown in Fig. 3, where we plot the residual on ϕ: $\phi^{\text{true}} - \phi^{\text{rec}}$. The vast majority of angles are reconstructed to better than 5 mrad. The tail in the resolution function corresponds to B decays with shorter decay lengths, where the vertex position error had a larger relative effect on the determination of ϕ. The slight asymmetry in the resolution function is an artefact of the resolution folded with the steeply-falling distribution of ϕ, which causes a small bias towards larger reconstructed vaues; this bias is explicitly corrected in the analysis (see below).

The double-inclusive distribution of raw B-hadron energies is shown in Fig. 4. Since we do not distinguish between B and $\overline{B}$ hadrons, the reconstructed B-decay vertices were labelled arbitrarily '1' and '2' on an event-by-event basis.

We divided E_B^{rec} by the beam energy, $E_{\text{beam}} = \sqrt{s}/2$, to obtain the reconstructed scaled B-hadron energy, $x_B^{\text{rec}} = E_B^{\text{rec}}/E_{\text{beam}}$.

4. Angle-dependent $B\overline{B}$ energy moments

In each event we quantified the correlations between the two B hadrons in terms of the angle de-

pendent scaled-energy moments proposed in [3]. Using the raw measured scale B energies we first evaluated the moments (Eq. (1)) from the raw measured distribution:

$$D_i^{\rm rec} = \frac{1}{2N}\Sigma_k \left(x_B^{\rm rec}\right)^{i-1}, \tag{11}$$

where the sum is over the set of reconstructed B hadrons and N is the number of events in the sample. Similarly, we evaluated in each $\cos\phi$ bin the double moments (Eq. (2))

$$D_{ij}^{\rm rec}(\phi) = \frac{1}{N}\Sigma_{N(\phi)} \left(x_{B1}^{\rm rec}\right)^{i-1} \left(x_{B2}^{\rm rec}\right)^{j-1}, \tag{12}$$

where the sum extends over the set of events in each $\cos\phi$ bin. The normalised moments G_{ij} (Eq. (3)) were evaluated:

$$G_{ij}^{\rm rec}(\phi) = \frac{D_{ij}^{\rm rec}(\phi)}{D_i^{\rm rec} D_j^{\rm rec}}. \tag{13}$$

The first six moments, $i = 1, 2, 3$ and $j = 1, \ldots, i$ are shown in Fig. 5. The bin centers were defined by taking the average value of $\cos\phi$ within each bin.

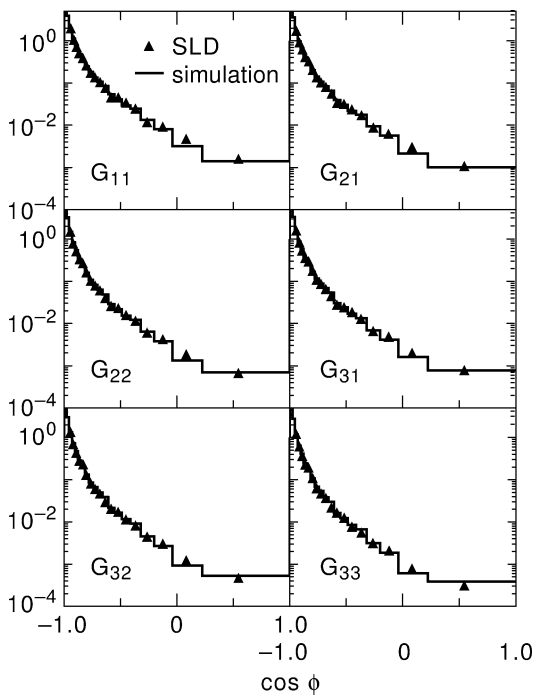

Fig. 5. Reconstructed moments of the two B-hadron energies (see text); the points include statistical error bars.

Also shown in Fig. 5 is a comparison with the simulated normalised moments; the simulation reproduces the data. Given that we showed previously [1,2] that the Peterson function implemented in our simulation does not provide a good description of the b-quark fragmentation function, this agreement may naively appear to be surprising. However, if, as proposed in [3], the non-perturbative contributions to the normalised quantity G_{ij} cancel, the agreement should be excellent, as observed.

We used our simulated event sample to correct for the effects of the detector acceptance, the efficiency of the technique for reconstructing B-hadron decays, the energy resolution, and bin migrations caused by the finite angular resolution. We defined a binwise correction factor:

$$F_{ij}^{\rm MC}(\phi) \equiv \frac{G_{ij}^{\rm gen}(\phi)|_{\rm MC}}{G_{ij}^{\rm rec}(\phi)|_{\rm MC}}, \tag{14}$$

where $G_{ij}^{\rm gen}(\phi)|_{\rm MC}$ is the normalised moment calculated using generated true $e^+e^- \to B\overline{B} + X$ events,

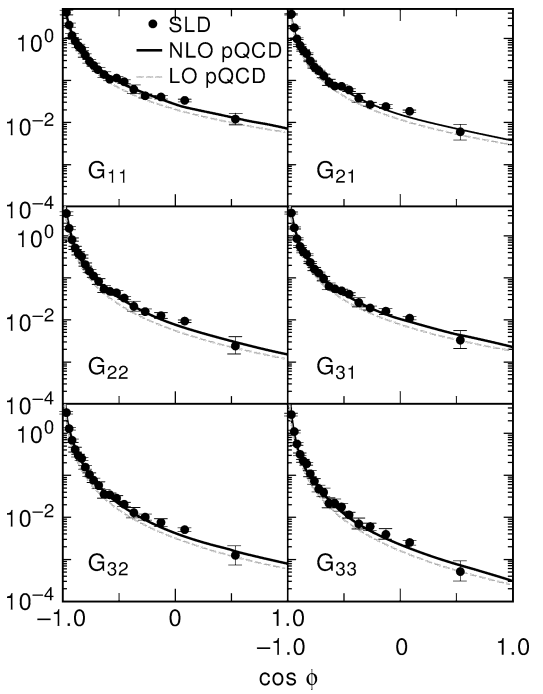

Fig. 6. Corrected moments of the two B-hadron energies compared with LO and NLO pQCD calculations. The error bars are the sum in quadrature of the statistical and systematic errors (see text).

and $G_{ij}^{\rm rec}(\phi)|_{\rm MC}$ is the corresponding moment calculated after simulation of the detector and application of the same analysis as applied to the data. For $\cos\phi \sim -1$ the value of F_{ij} is close to unity. As $\cos\phi$ increases towards 1, F_{ij} rises monotonically to approximately 8 (F_{11}) or 2 (F_{33}). The increase with $\cos\phi$ reflects our decreasing efficiency to select $B\overline{B}$ events as the angle between the two B-decay vertices becomes smaller and the B energies decrease. For a given $\cos\phi$ bin, F_{ij} decreases as i and j increase due to the effective weighting of this efficiency by $x_B^{i-1}x_B^{j-1}$.

We derived the true normalised moments:

$$G_{ij}(\phi) = F_{ij}^{\rm MC}(\phi)G_{ij}^{\rm rec}(\phi) \tag{15}$$

which are shown in Fig 6. The uncertainties associated with this correction procedure are discussed in the next section.

5. Error estimation

Since it is not possible to calculate them analytically, we used our simulation to estimate the statistical error on the moments. The simulated event sample was divided into subsamples, each comprising the same number of events as in the data sample. The entire analysis was performed on each of these subsamples. Within each $\cos\phi$ bin the r.m.s. deviation of the ensemble of results was evaluated and taken as the statistical error in that bin. For a given pair of i and j values the errors on the particular moment are not correlated between different bins of $\cos\phi$, but within a given $\cos\phi$ bin the errors on the different moments are correlated, since the same set of events was used.

We considered sources of systematic uncertainty that potentially affect our measurements. These may be divided into uncertainties in modeling the detector and uncertainties on experimental measurements serving as input parameters to the underlying physics modeling. For these studies our simulation was used.

Since our energy reconstruction technique is strongly dependent on charged-track properties, four sources of uncertainty were investigated: our simulated tracking efficiency, transverse momentum resolution, and the resolutions on the track impact parameter and polar angles. In each case the simulation was corrected so as to reproduce the data. The full analysis was repeated on the data, and half the difference between the results obtained using the corrected and uncorrected simulations was taken as a symmetric systematic error.

A large number of measured quantities relating to the production and decay of charm and bottom hadrons are used as input to our simulation. In $b\bar{b}$ events we considered the uncertainties on: the branching fraction for $Z^0 \to b\bar{b}$; the rates of production of $B^{\pm}$, B^0 and B_s^0 mesons, and B baryons; the lifetimes of B mesons and baryons; and the average B-hadron decay charged multiplicity. In $c\bar{c}$ events we considered the uncertainties on: the branching fraction for $Z^0 \to c\bar{c}$; the charmed hadron lifetimes, the charged multiplicity of charmed hadron decays, the production of K^0 from charmed hadron decays, and the fraction of charmed hadron decays containing no π^0s. We also considered the rates of production of secondary $b\bar{b}$ and $c\bar{c}$ from gluon splitting. The uncertainty on the world-average value [2] of each quantity was used to rederive the corrected $G_{ij}(\phi)$. In each bin of $G_{ij}(\phi)$ the deviation between the rederived and standard values was taken as an estimate of the corresponding systematic error. Other relevant systematic effects such as variation of the event selection cuts and the assumed B-hadron mass were found to be very small.

The error associated with the choice of b-quark fragmentation function used in the simulation was estimated by rederiving the corrected data using in turn the UCLA, Kartvelishvili and Bowler fragmentation functions [2]. In each $\cos\phi$ bin the r.m.s. deviation of the results w.r.t. the standard value, using the Peterson function, was taken as an estimate of the systematic error. This error was typically much smaller than that arising from the other error sources.

For each systematic error investigated, the shape of the angular dependence of the moments was not significantly changed, only the overall normalization was affected. For each moment, in each $\cos\phi$ bin the dominant errors were typically those related to the uncertainties on the charged-track properties. The errors due to charm and bottom physics modeling were typically an order of magnitude smaller. In each $\cos\phi$ bin all sources of systematic uncertainty were added in quadrature to obtain the total systematic error. The fully-corrected G_{ij}, with statistical and systematic errors added in quadrature, are shown in Fig. 6.

6. Comparison with perturbative QCD calculations

The fully-corrected data [16] were compared (Fig. 6) with a recent calculation [4] of the normalised moments complete at NLO in pQCD. Both the LO and full NLO calculations are shown in Fig. 6; the calculations assume an $\alpha_s(M_Z^2)$ value of 0.120 and a pole b-quark mass value of 5.0 GeV/c^2.[2] It can be seen that the difference between the two is relatively small, and that the LO calculation lies systematically slightly below the NLO calculation. The small size of the NLO relative to the LO contributions is an indication that the normalised moments are perturbatively robust observables. For each moment shown, the LO calculation undershoots the data. The NLO calculation reproduces the data across the full range of $\cos\phi$.

This comparison does not rely on any convolution of the pQCD calculations with models of the non-perturbative hadronisation process. Hence the excellent agreement between the pQCD calculations and the data verifies the ansatz of factorization between the perturbative and non-perturbative phases that forms the basis for the pQCD calculation of heavy-hadron properties.

Acknowledgements

We thank the personnel of the SLAC accelerator department and the technical staffs of our collaborating institutions for their outstanding efforts on our behalf. We thank A. Brandenburg, P. Nason and C. Oleari for helpful discussions.

References

[1] SLD Collaboration, K. Abe, et al., Phys. Rev. Lett. 84 (2000) 4300.
[2] SLD Collaboration, K. Abe, et al., Phys. Rev. D 65 (2002) 092006.
[3] P.N. Burrows, P. Hoyer, V. Del Duca, Z. Phys. C 53 (1992) 149.
[4] A. Brandenburg, P. Nason, C. Oleari, hep-ph/0304272.
[5] SLD Design Report, SLAC Report 273 1984.
[6] SLD Collaboration, K. Abe, et al., Phys. Rev. D 51 (1995) 962.
[7] M.D. Hildreth, et al., IEEE Trans. Nucl. Sci. 42 (1994) 451.
[8] C.J.S. Damerell, et al., Nucl. Instrum. Methods A 400 (1997) 287.
[9] S. Brandt, et al., Phys. Lett. 12 (1964) 57;
E. Farhi, Phys. Rev. Lett. 39 (1977) 1587.
[10] T. Sjöstrand, Comput. Phys. Commun. 82 (1994) 74.
[11] P.N. Burrows, Z. Phys. C 41 (1988) 375;
OPAL Collaboration, M.Z. Akrawy, et al., Z. Phys. C 47 (1990) 505.
[12] SLD Collaboration, K. Abe, et al., Phys. Rev. Lett. 79 (1997) 590.
[13] R. Brun, et al., Report No. CERN-DD/EE/84-1 (1989).
[14] D.J. Jackson, Nucl. Instrum. Methods A 388 (1997) 247.
[15] D. Dong, PhD thesis, Massachusetts Institute of Technology, SLAC-Report-550, 1999.
[16] G. Nesom, PhD thesis, University of Oxford, 2003.
[17] N. Brown, W.J. Stirling, Z. Phys. C 53 (1992) 629.

[2] Variation of the pole b-quark mass within the Particle Data Group range, 4.6–5.1 GeV/c^2, changes the theoretical prediction by at most 1%. This is small compared with, for example, the change due to the uncertainty on $\alpha_s(M_Z^2)$.